Theoretical studies on mechanism and kinetics of the hydrogen-abstraction reaction of CF3C(O)OCH2CH3 with OH radicals

ARTICLE *in* COMPUTATIONAL AND THEORETICAL CHEMISTRY · JANUARY 2013

Impact Factor: 1.55 · DOI: 10.1016/j.comptc.2013.12.019

4 AUTHORS, INCLUDING:

Hui Wang
Chinese Academy of Sciences
17 PUBLICATIONS **63** CITATIONS
SEE PROFILE

Jing-Yao Liu
Jilin University
148 PUBLICATIONS **736** CITATIONS
SEE PROFILE

Computational and Theoretical Chemistry 1029 (2014) 91–98

Contents lists available at ScienceDirect

Computational and Theoretical Chemistry

journal homepage: www.elsevier.com/locate/comptc

Theoretical studies on mechanism and kinetics of the hydrogen-abstraction reaction of $CF_2HCOOCH_3$ with OH radicals

Peng Zhu, Li-ling Ai, Hui Wang, Jing-yao Liu *

State Key Laboratory of Theoretical and Computational Chemistry, Institute of Theoretical Chemistry, Jilin University, Changchun 130023, PR China

ARTICLE INFO

Article history:
Received 16 September 2013
Received in revised form 16 December 2013
Accepted 17 December 2013
Available online 29 December 2013

Keywords:
Direct dynamics method
Rate constant
Variational transition-state theory
Density functional theory
Hydrogen abstraction

ABSTRACT

The hydrogen abstraction reaction of $CF_2HCOOCH_3$ + OH has been studied theoretically by a dual-level direct dynamics method. The geometries and frequencies of all stationary points are optimized at the M06-2X/aug-cc-pVDZ level, and the energy profile is refined with interpolated single-point energy (ISPE) by the MCG3-MPWB method. Two stable conformers of $CF_2HCOOCH_3$ are located, and for each conformer, the possible H-abstraction channels from $-CH_3$ and $-CF_2H$ groups are taken into account. The rate constants are calculated using the improved canonical variational transition-state theory (ICVT) with the small-curvature tunneling correction (SCT) and are fitted by a three-parameter Arrhenius equation over a wide temperature range. Due to the lack of the kinetic data of these reactions, the present theoretical results are expected to be useful and reasonable to estimate the kinetic data of the reaction over a wide temperature range where no experimental value is available.

1. Introduction

Due to the adverse effect on the depletion of the stratospheric ozone layer and global warming caused by chlorofluorocarbons (CFCs), a number of replaceable compounds have been considered as substitutes for CFCs in various applications. Hydrofluoroethers (HFEs), which have similar physical and chemical properties to CFCs and contain neither chlorine nor bromine atoms, have been suggested as a new class of CFCs substitutes from the point of view of ozone depletion [1–4]. Moreover, due to the introduction of ether linkage –O–, HFEs are expected to have greater reactivity and shorter atmospheric lifetimes in the troposphere. The oxidation reactions of HFEs are mainly proceed via hydrogen abstraction by OH radicals, followed by the addition of O_2 to form a peroxy radical, which reacts further to ultimately generate the homologous hydrofluorinated esters (FESs) [5–7]. Thus, FESs are the primary atmospheric oxidation products of HFEs. FESs possess zero ozone depletion potentials (ODP), however, they still may contribute to global warming due to containing numerous C–F bonds, which can adsorb IR radiation. Similar to the HFEs, the FESs' lifetimes are mainly determined by the reactions with OH radicals [8,9], since the reactions with other chemical species like chlorine atoms and wet depositions in the clouds are less important in their loss process in the atmosphere. Therefore, in order to assess the environmental impact in air pollution and the global warming, quantitative kinetic data and degradation mechanism information for the OH radical initiated oxidation reactions of FESs are required.

Unfortunately, the information on the kinetics and mechanisms of FESs towards OH radicals is rather limited. In the present work, we focus on the reaction of methyl difluoroacetate ($CF_2HCOOCH_3$) with OH radicals. The kinetic study for this reaction was performed using the relative technique by Blanco and Teruel [8], and the rate constant was measured only at the temperature of 298 K, with a value of $(1.48 \pm 0.34) \times 10^{-13}$ cm^3 molecule^{-1} s^{-1}. With respect to the reactant $CF_2HCOOCH_3$, two stable conformers are located, denoted as conformer I with C_s symmetry and conformer II with C_1 symmetry (see Fig. 1). Based on our theoretical calculation, the energy difference between the two conformers is only within 0.5 kcal mol^{-1}. Also, for each conformer, the hydrogen atom can be abstracted from either $-CF_2H$ or $-CH_3$ site, and thus more than one reaction channel may be possible. However, it is difficult to determine which hydrogen atom can be abstracted and which conformer has main contribution to the overall reaction in experiment. So in view of the lack of the kinetic study for this reaction, it is very desirable to perform a detailed theoretical study to provide a deep insight into the reaction mechanism, and predict the rate constants and the branching ratios over a wide temperature range.

In the present work, we performed dual-level (*X*//*Y*) direct dynamics calculations [10–12] to investigate the kinetic nature of the title reaction. The required potential energy surface (PES) information for the kinetic calculations is obtained directly from the electronic structure calculations, in which the M06-2X density functional method [13] is used to optimize all the stationary points

* Corresponding author. Fax: +86 431 88498026.
E-mail addresses: ljy121@jlu.edu.cn, jingyao121@gmail.com (J.-y. Liu).

2210-271X/$ - see front matter © 2013 Elsevier B.V. All rights reserved.
http://dx.doi.org/10.1016/j.comptc.2013.12.019

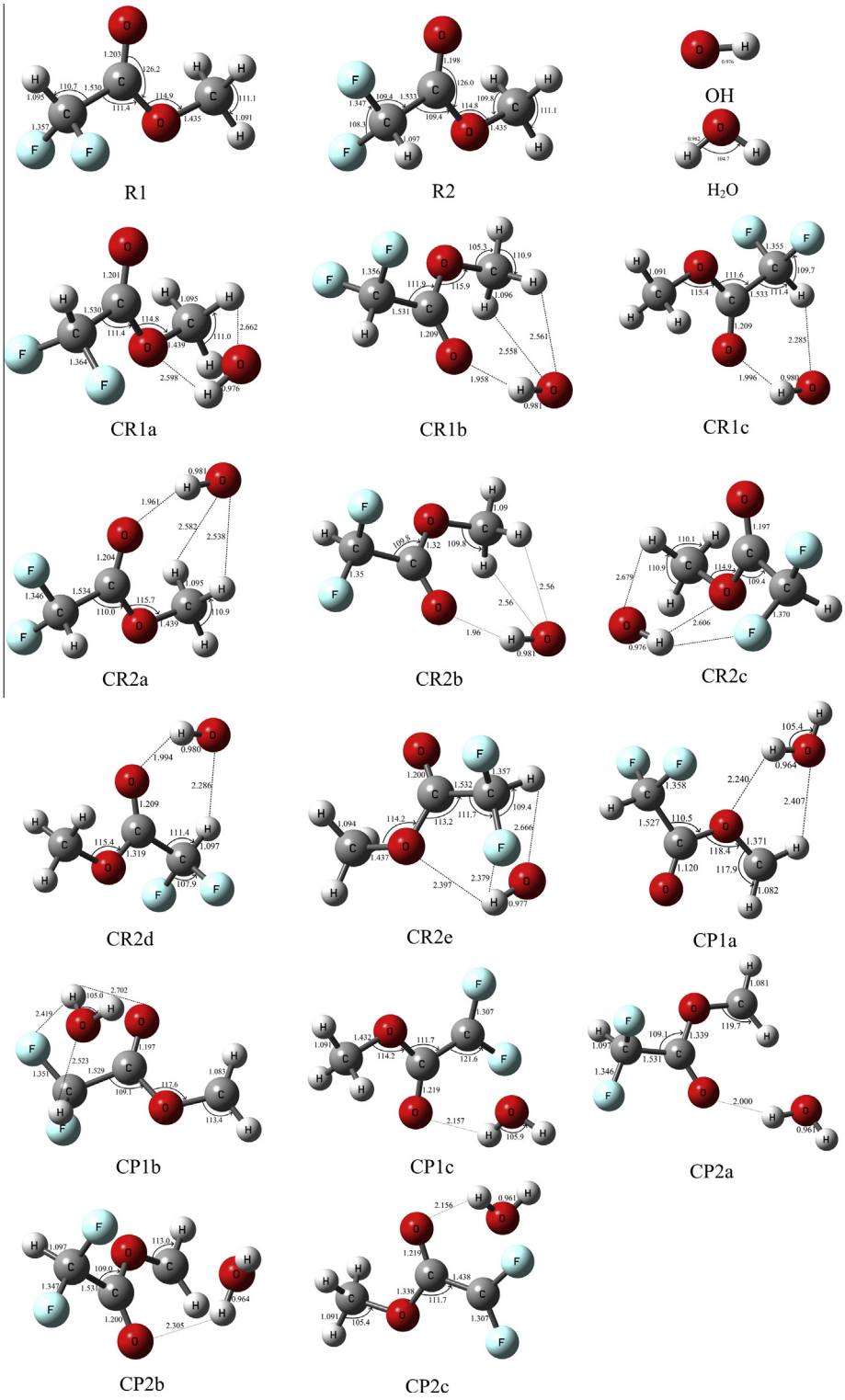

Fig. 1. Optimized geometry parameters of reactants, products, transition states, and hydrogen-bond complexes at the M06-2X/aug-cc-pVDZ. Experimental values [31] are given in parentheses. Bond lengths are in angstroms and angles are in degree.

on the PES and multilevel MCG3-MPWB method [14] is used to refine the high-level single-point energies at the M06-2X geometries. The rate constants for each channel are evaluated using variational transition-state theory (VTST) [15–17] with interpolated single-point energies (ISPE) [18] approach. The site selectivity of the potential reaction sites and the contribution of each conformer to the overall reaction are discussed.

2. Computational methods

In the present study, all of the electronic structure calculations are carried out with the Gaussian 09 program [19]. The optimized geometries and harmonic vibrational frequencies of all the stationary points (reactants, hydrogen-complexes, transition states, and products) are calculated using the M06-2X method with the

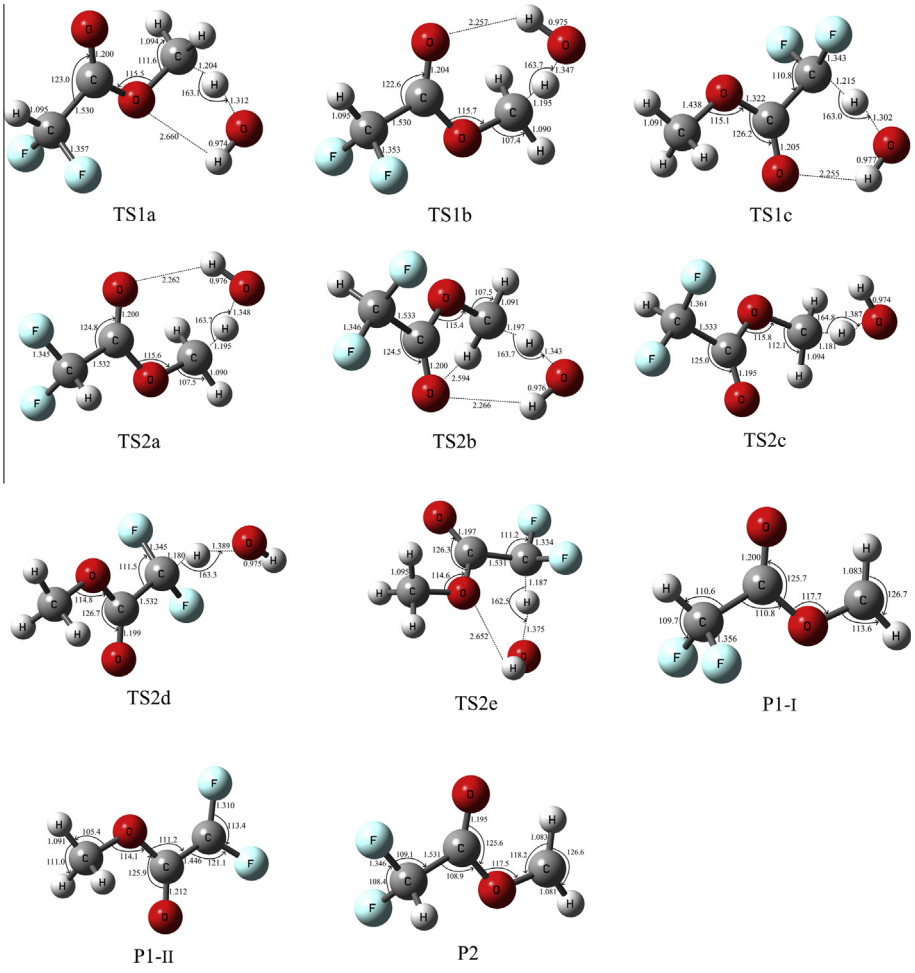

Fig. 1 (*continued*)

aug-cc-pVDZ basis set (M06-2X/aug-cc-pVDZ). At the same level, the minimum-energy path (MEP) is calculated by the intrinsic reaction coordinate (IRC) theory to confirm that the transition state really connects with minima along the reaction path. Also, the energy derivatives, including gradients and Hessians at geometries along the MEP, are obtained. To calculate the curvature of the reaction path and the generalized vibrational frequencies along the reaction path, single-point energy calculations for the stationary points and four extra points along the MEP are carried out by the multicoefficient extrapolated density functional method MCG3-MPWB.

The initial information on the PES is put into the POLYRATE 9.7 program [20], and then the kinetic calculations for reactions R1 and R2 are calculated by using the variational transition-state theory (VTST) with the interpolated single-point energy (ISPE) method. The ISPE method is a dual-level direct dynamics scheme, in which for each channel four extra energies calculated at a high-level of theory along the low-level MEP are used to correct the classical energetic profile of the reaction. The rate constants are calculated using the improved canonical variational transition-state theory (ICVT) [21], and the tunneling correction is considered by the small-curvature tunneling (SCT) correction [22,23], which has been successfully used in the studies for many H-abstraction reactions [24–29]. In the calculation of the electronic partition function, two electronic states for OH radical, with a 140 cm^{-1} splitting in the $^2\prod$ ground state, are included.

An accurate knowledge of the enthalpy of formation of the species is important in determining the thermodynamic properties and the kinetics of atmospheric processes. However, there is little data on the species $CF_2HCOOCH_3$, $CF_2HCOOCH_2$, and CF_2COOCH_3 experimentally or theoretically. In this work, the enthalpies of formation of species are estimated by using isodesmic reactions [30]. Because of the conservation of the number of electron pairs between reactants and products and the similarity of bond type, these reactions will cancel the systematic errors in the calculations and lead to relative accurate results. Here, we predict the enthalpies of formation of the reactant $CF_2HCOOCH_3$ and product radicals $CF_2HCOOCH_2$ and CF_2COOCH_3 using the following isodesmic reactions:

$$CF_2HCOOCH_3 + CH_4 \rightarrow CH_2F_2 + CH_3COOCH_3 \quad (I)$$

$$CF_2HCOOCH_2 + CH_2F_2 + CH_4 \rightarrow CF_4 + CH_3 + CH_3COOCH_3 \quad (II)$$

$$CF_2COOCH_3 + CH_2F_2 + CH_4 \rightarrow CF_3 + CH_3F + CH_3COOCH_3 \quad (III)$$

The electronic structure calculations of above three reactions are also performed at the same MCG3-MPWB//M06-2X/aug-cc-pVDZ level.

3. Results and discussions

3.1. Stationary points

The geometric parameters of all the stationary points involved in reactions R1 and R2 optimized at the M06-2X/aug-cc-pVDZ level

are displayed in Fig. 1, along with the available experimental data [31] of OH and H_2O. The harmonic vibrational frequencies are calculated at the same level of theory to characterize the nature of each critical point and to make zero-point energy (ZPE) corrections. The calculated frequencies are listed in Table S1. All of the reactants, products and complexes have only real frequencies, while the transition states are identified by normal-mode analysis to have only one imaginary frequency corresponding to the coupling of the breaking C–H bond and the forming O–H bond stretching vibrational modes. With respect to reactant $CF_2HCOOCH_3$, two stable conformers (I, II), one with C_s symmetry (conformer I) and the other with C_1 symmetry (conformer II), are identified. The two conformers with the H–C–C–O dihedral angles of 54.8° and 0°, respectively, can transform to each other by the rotation of the $-CF_2H$ group. The C_s conformer is found to be more stable than the C_1 conformer by about 0.39 kcal mol^{-1} at the M06-2X/aug-cc-pVDZ level and 0.48 kcal mol^{-1} at the MCG3-MPWB//M06-2X/aug-cc-pVDZ level. The small energy difference between them implies that both of them may have contribution to the title reaction by weight factors estimated from Boltzmann distribution function.

Two kinds of hydrogen abstractions can occur from the $-CH_3$ and $-CF_2H$ groups for both of the C_s and C_1 conformers. As for the reactant with C_s symmetry, the two out-of-plane hydrogen atoms of the $-CH_3$ group are equivalent, while the in-plane hydrogen atom represents another alternative for H-abstraction. Therefore, three H-abstraction channels, two from $-CH_3$ group and one from $-CF_2H$ group, are feasible, denoted as R1a, R1b and R1c.

$$CF_2HCOOCH_3\ (I) + OH \rightarrow CF_2HCOOCH_2 + H_2O \quad (R1a \text{ and } R1b)$$

$$CF_2HCOOCH_3\ (I) + OH \rightarrow CF_2COOCH_3 + H_2O \quad (R1c)$$

In the case of C_1 conformer, since the three hydrogen atoms in the $-CH_3$ group are not equivalent, there are three distinguished H-abstractions channels (denoted as R2a, R2b, and R2c) from $-CH_3$ group; and for the H-abstractions from $-CF_2H$ group, two distinguished H-abstractions channels (denoted as R2d and R2e) are located, depending on the different –OH attacking orientations. All the five distinguished channels are represented as follows:

$$CF_2HCOOCH_3\ (II) + OH \rightarrow CF_2HCOOCH_2 + H_2O \quad (R2a, R2b \text{ and } R2c)$$

$$CF_2HCOOCH_3\ (II) + OH \rightarrow CF_2COOCH_3 + H_2O \quad (R2d \text{ and } R2e)$$

Because of the high electronegativity of the fluorine and oxygen atoms, the hydrogen-bonded complexes with energy less than those of the reactants or products are located at the entrance or exit of each channel, which means that the reaction may proceed via an indirect mechanism. In the complexes, the hydrogen-bond lengths of O...H and H...F are all less than the sum of their van der Waals radii (2.72 and 2.67 Å), and the other bond lengths are very close to those of reactants or products. It is seen that the structures of TSs look more similar to those of reactants than to those of products. For example, in TS1a the breaking bond C–H is elongated by about 9% in comparison to the C–H equilibrium bond length in the isolated $CF_2HCOOCH_3$ (I) and the forming O–H bond is elongated by 36% longer than the regular bond length of the isolated H_2O. The elongation of the forming bond (O–H) is greater than that of the breaking bond (C–H), which indicates that the transition state is reactant-like, and the reaction may proceed via an "early" transition state for the exothermic reaction. Similar conclusion can be drawn from the other TSs. In addition, the intramolecular hydrogen bonds interaction between O and H (Fig. 1a) exist in some TSs, which may stabilize the corresponding TS structure. For example, with respect to the three H-abstraction TSs from $-CH_3$ group of $CF_2HCOOCH_3$ (II), intramolecular hydrogen bonds are found in TS2a and TS2b but not in TS2c, which indicates that TS2a and TS2b may be more stable than TS2c. Moreover, for the two H-abstraction TSs (TS1a and TS1b) from $-CH_3$ group of $CF_2HCOOCH_3$ (I), although the hydrogen bonds exist in both of TS1a and TS1b, the hydrogen bond length in TS1b (2.257 Å) is shorter than that in TS1a (2.660 Å), which suggests that the H-bond interaction in TS1b is stronger than that in TS1a, and as a result, TS1b may have a lower energy than TS1a. These predictions will be confirmed by energy comparison in the next section.

Table 1
The standard enthalpies of formation ($\Delta H^o_{f,298}$) (in kcal mol^{-1}) at 298 K calculated at the MCG3-MPWB//M06-2X/aug-cc-pVDZ level.

Species	$\Delta H^o_{f,298}$	Species	$\Delta H^o_{f,298}$
$CF_2HCOOCH_2$ (I)	−249.14	$CF_2HCOOCH_3$ (II)	−248.56
$CF_2HCOOCH_2$ (I)	−200.91	$CF_2HCOOCH_3$ (II)	−200.44
CF_2COOCH_3	−206.06		

3.2. Energetics

The enthalpies (ΔH^o_{298}) at 298 K of the reaction are calculated at the MCG3-MPWB//M06-2X/aug-cc-pVDZ level. All of the reaction channels are exothermic, with the (ΔH^o_{298}) values of −19.3 kcal mol^{-1} (for R1a and R1b), −23.8 kcal mol^{-1} (for R1c), −19.3 kcal mol^{-1} (for R2a, R2b and R2c) and −24.4 kcal mol^{-1} (for R2d and R2e). Because of lack of the experimental enthalpies ($\Delta H^o_{f,298}$) of the reactant and product radicals, a direct comparison between theoretical and experimental results of the reaction enthalpies is not available. It is well known that an accurate knowledge of the enthalpies of formation (ΔH^o_{298}) for species is required for a thorough understanding of the kinetics and mechanisms of their reactions, particularly in atmospheric modeling. Here the (ΔH^o_{298}) values of both I and II conformers of $CF_2HCOOCH_3$, CF_2COOCH_3 and $CF_2HCOOCH_2$ are obtained by using the calculated reaction enthalpies of the isodesmic reactions (I)–(III) and the experimental (ΔH^o_{298}) of the other species involved in the reactions (CH_2F_2, −107.66 kcal mol^{-1} [31]; CH_4, −17.9 kcal mol^{-1} [31]; CF_4, −222.17 kcal mol^{-1} [31]; CH_3F, −55.97 kcal mol^{-1} [31]; CH_3, 34.81 kcal mol^{-1} [31]; CF_3, −112.35 kcal mol^{-1} [31]; CH_3COOCH_3, −97.95 kcal mol^{-1} [31]). The enthalpies of formation calculated at the MCG3-MPWB//M06-2X level are −249.14, −248.56, −200.91, −200.44 and −206.06 kcal mol^{-1} for $CF_2HCOOCH_3$ (I), $CF_2HCOOCH_3$ (II), $CF_2HCOOCH_2$ (I), $CF_2HCOOCH_2$ (II) and CF_2COOCH_3, respectively, which are presented in Table 1.

Schematic potential energy diagrams of the reaction of $CF_2HCOOCH_3$ (I, II) with OH obtained at the MCG3-MPWB//M06-2X/aug-cc-pVDZ level with the ZPE corrections are plotted in Fig. 2a and b, respectively. The energy of the reactants is set to zero for reference. For the reaction channels of R1, the hydrogen-bonded complexes CR1a, CR1b and CR1c are located at the entrance channels with the energies of CR1a, CR1b and CR1c −0.7, −3.3, and −3.1 kcal mol^{-1}, respectively. Starting from this pre-reactant complex, each reaction passes through a reactant-like transition state to form another hydrogen-bonded complex at the product side. The relative energies of CP1a, CP1b and CP1c are 1.5, 2.9, and 2.5 kcal mol^{-1} below the corresponding products. Fig. 2a shows that the energy barrier of the reaction R1b is the lowest one among the three channels of $CF_2HCOOCH_3$ (I) + OH, lower than that of R1a by 2.8 kcal mol^{-1}, as can be attributed by the stronger H-bond interaction. Similarly, seen from Fig. 2b, we can see that for channels R2a–R2e, five reactant complexes are first formed with energies about −3.4, −3.6, −2.1, −3.7 and −0.7 kcal mol^{-1} lower than the reactants. Then starting from the complexes, each of the

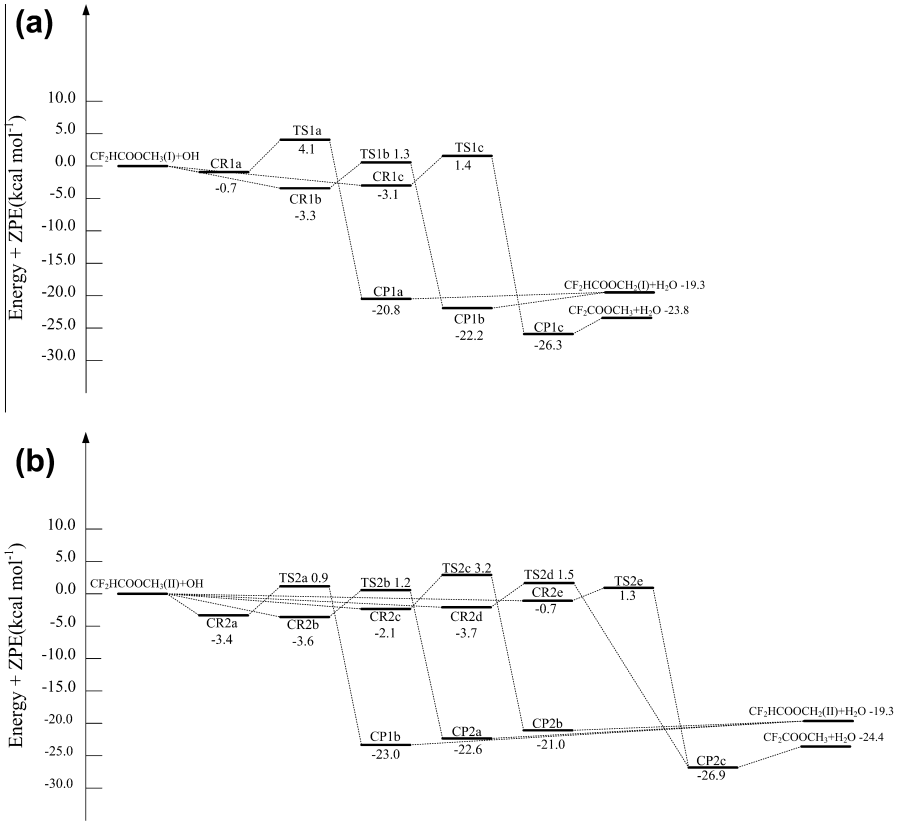

Fig. 2. Schematic potential energy surfaces (a) for the $CF_2HCOOCH_2$ (I) + OH reaction, (b) for the $CF_2HCOOCH_3$ (II) + OH reaction. Relative energies with ZPE at the MCG3-MPWB//M06-2X/aug-cc-pVDZ level are in kcal mol^{-1}.

reaction passes through a reactant-like TS to form another product complex, which lies below the corresponding products. As seen from Fig. 2b, the barrier heights of R2a, R2b, R2c (H-abstraction from $-CH_3$ position), R2d and R2e (H-abstraction from $-CF_2H$ position) are 0.9, 1.2, 3.2, 1.5 and 1.3 kcal mol^{-1}, respectively. For H-abstraction from $-CH_3$ position, the energy barrier of the reaction R2c is lower than that of R2a and R2b by about 2.3 and 2.0 kcal mol^{-1}, respectively, which can be attributed to the existence of the intramolecular hydrogen bonds in TS2a and TS2b. The exothermic values of R2a, R2b and R2c (H-abstraction from $-CH_3$ position) are less than other two channels R2d and R2e (H-abstraction from $-CF_2H$ group) by about 5.1 kcal mol^{-1}, so the reaction (R2d and R2e) may be thermodynamically more favorable than (R2a, R2b and R2c). Thus, according to the comparison of the barrier height and the reaction enthalpy, we can conclude that the reactions taking place from $-CH_3$ group may be competitive with the reactions taking place from $-CF_2H$ group over the whole temperature range.

4. Rate constant calculation

Dual-level kinetic calculations of the hydrogen abstraction reactions R1 and R2 are carried out with VTST-ISPE approach, in which four extra MCG3-MPWB//M06-2X/aug-cc-pVDZ energies are used to refine the classical energy profile. The rate constants are calculated by conventional transition-state theory (TST), the TST with zero-curvature tunneling (ZCT) correction, the improved canonical variational transition-state theory (ICVT), and ICVT with the small-curvature tunneling (SCT) correction over the temperature range from 200 to 1000 K. The TST, ICVT and ICVT/SCT rate constants for channels R1b and R2e are presented in Fig. 3a and b, respectively, while those for other channels are given in Supporting information Fig. S1 (a–f). As seen from Fig. 3a, the TST and ICVT rate constants of channel R1b are nearly the same over the whole temperature range, which means that the variational effect is very small. Similar cases can be found for the channels of R1a, R1c, R2a and R2b. While for R2e, the ratios of k_{ICVT}/k_{TST} are 0.89 at 298 K and 0.76 at 500 K, which indicates that the variational effect is important to the rate constants for this channel. Similar conclusions can be drawn from R2c and R2d (see Fig. S1e and S1f). On the other hand, by comparing the ICVT and ICVT/SCT values, we find that the SCT correction is very small for R2d and R2e while plays an important role in the rate constant calculations for other channels at low temperature. For example, the ratios of $k_{ICVT/SCT}/k_{ICVT}$ for R2e and R1b are 1.2 and 3.8 at 200 K, respectively. However, as temperature increases, it is seen that the tunneling effect for all channels is almost negligible. In addition, for comparison, the TST/ZCT rate constants for channel R1b (with almost no variational effect) are also shown in Fig. 3a. It can be seen the TST/ZCT values are smaller than the ICVT/SCT values at the whole temperatures; for example, the $k_{TST/ZCT}/k_{ICVT/SCT}$ ratios are 0.62 at 200 K and 0.76 at 298 K. These results indicate it is very necessary to perform the VTST calculations for this system.

The total rate constants for reactions R1 and R2 is obtained from the sum of the individual ICVT/SCT results associated with the available reaction paths ($k_1 = k_{1a} + k_{1b} + k_{1c}$ and $k_2 = k_{2a} + k_{2b} + k_{2c} + k_{2d} + k_{2e}$). The temperature dependence of the branching ratios of R1 and R2 is exhibited in Fig. 4a and b. Fig. 4a shows that R1b is the dominant channel of R1, and R1c is the second competitive one, while R1a is the least one at low temperature. For example, the ratios of k_{1b}/k_1 and k_{1c}/k_1 are 0.76 and 0.24 at 200 K, respectively. However, as the temperature increases, the ratio of

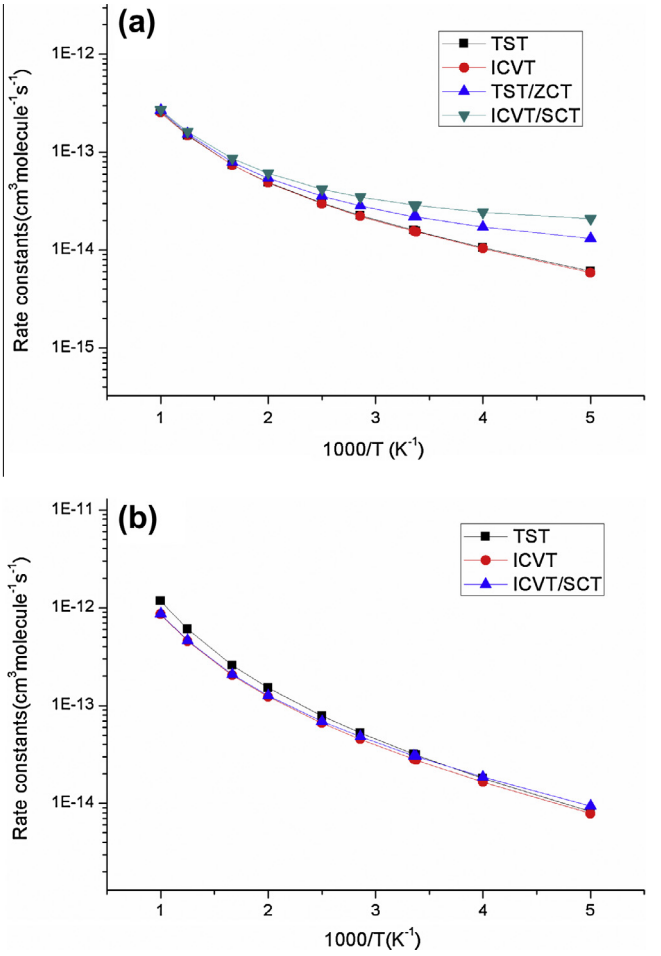

Fig. 3. The TST, ICVT and ICVT/SCT rate constants calculated at the MCG3-MPWB//M06-2X/aug-cc-pVDZ level versus 1000/*T* between 200 and 1000 K: (a) for R1b, (b) for R2e.

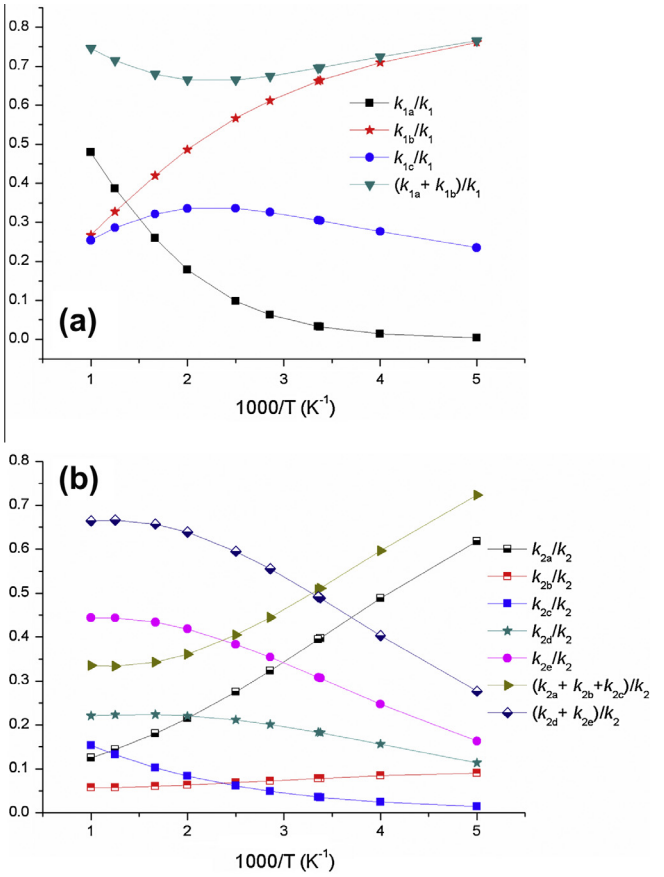

Fig. 4. Plots of the calculated branching ratios versus 1000/*T* between 200 and 1000 K (a) for the reaction $CF_2HCOOCH_3$ (I) + OH → products and (b) for the reaction $CF_2HCOOCH_3$ (II) + OH → products.

k_{1a}/k_1 increases while the one of k_{1b}/k_1 decreases and the former becomes larger than the latter at high temperature. For example, the ratios of k_{1a}/k_1 and k_{1b}/k_1 are 0.48 and 0.27 at 1000 K, respectively. This indicates R1a becomes the major channel at high temperature. On the other hand, since the three H-atoms in the $-CH_3$ group are indistinguishable, it is fond that the contribution from the $-CH_3$ group, i.e., $k_{CH3} = k_{1a} + k_{1b}$ to the overall reaction is more important than that from the $-CF_2H$ group, i.e., k_{1c} at the whole temperature range (as shown in Fig. 4a). For the reaction of $CF_2HCOOCH_3$ (II) + OH, in the low temperature range, the contribution of channel R2a to the total rate constant is more important than that of R2b, R2c, R2d and R2e. For example, the ratio of k_{2a}/k_2 is 0.72 at 200 K. However, as the temperature increases, channel R2e become comparable to R2a and more important to the total reaction; the ratios of k_{2a}/k_2 and k_{2e}/k_2 are 0.29 and 0.38 at 400 K and 0.12 and 0.44 at 1000 K. Seen from Fig. 4b, the contribution from the $-CH_3$ group, i.e., $k_{CH3} = k_{2a} + k_{2b} + k_{2c}$ to R2 is more important than that from the $-CF_2H$ group, i.e., $k_{CF2H} = k_{2d} + k_{2e}$ at low temperature range, with the k_{CH3}/k_2 and k_{CF2H}/k_2 ratios of 0.72 and 0.28 at 200 K, respectively. However, different from R1, as the temperature increases, H-abstractions from $-CF_2H$ group become more favorable than those from $-CH_3$ group and the corresponding ratios of k_{CH3}/k_2 and k_{CF2H}/k_2 are 0.34 and 0.66 at 1000 K, respectively. In all cases, we can conclude that H-abstractions from the $-CH_3$ group in the two conformers of $CF_2HCOOCH_3$ are the major reaction channels at the low temperature range.

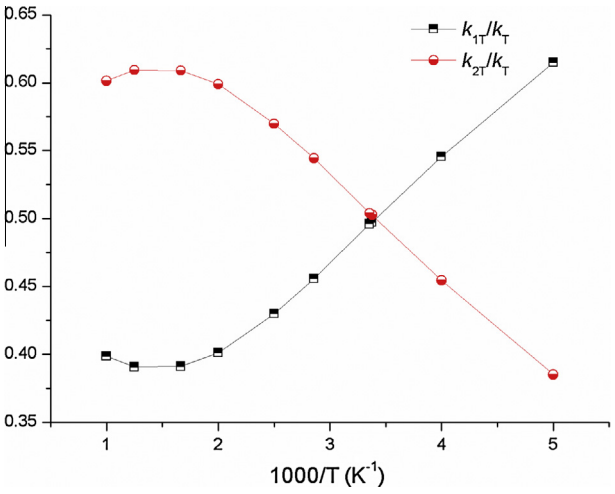

Fig. 5. Plot of the contributions of $CF_2HCOOCH_3$ (I) and $CF_2HCOOCH_3$ (II) to the reaction versus 1000/*T* between 200 and 1000 K.

The overall rate constant ($k_{overall}$) for the title reaction of $CF_2HCOOCH_3$ + OH can be obtained from the following expression,

$$K_{overall} = \omega_1 k_1 + \omega_2 k_2$$
$$= \omega_1(k_{1a} + k_{1b} + k_{1c}) + \omega_2(k_{2a} + k_{2b} + k_{2c} + k_{2d} + k_{2e})$$
$$= k_{1T} + k_{2T}$$

where ω_1 and ω_2 are the weight factors of each conformer calculated from the Boltzmann distribution function. From this

Table 2
Rate constants (in cm^3 $molecule^{-1}$ s^{-1}) as well as weight factors for each conformer and the overall rate constant ($k_{overall}$) (in cm^3 $molecule^{-1}$ s^{-1}) in the temperature range 200–1000 K at the MCG3-MPWB//M06-2X level.

T (K)	k_1	ω_1	k_2	ω_2	k_T	Exptl.
200	2.75E−14	0.770	5.77E−14	0.230	3.44E−14	
250	3.42E−14	0.725	7.49E−14	0.275	4.54E−14	
296	4.30E−14	0.694	9.83E−14	0.306	5.99E−14	
298	4.34E−14	0.692	9.93E−14	0.308	6.06E−14	(1.48 ± 0.34) E−13[a]
350	5.68E−14	0.666	1.35E−13	0.334	8.30E−14	
400	7.41E−14	0.647	1.80E−13	0.353	1.11E−13	
500	1.25E−13	0.619	3.03E−13	0.381	1.93E−13	
600	2.06E−13	0.599	4.80E−13	0.401	3.16E−13	
800	4.93E−13	0.575	1.04E−12	0.425	7.26E−13	
1000	1.01E−12	0.560	1.95E−12	0.440	1.43E−12	

[a] From Ref. [8].

expression, it is easy to evaluate what degree of each conformer contributes to the overall rate constant. For example, the ω_1 and ω_2 are 0.77 and 0.23 at 200 K and 0.56 and 0.44 at 1000 K, respectively. In addition, the contributions of $CF_2HCOOCH_3$ (I) and $CF_2HCOOCH_3$ (II), $k_{1T}/k_{overall}$ and $k_{2T}/k_{overall}$, to this reaction are plotted in Fig. 5. It is seen that below 290 K, the contribution of $CF_2HCOOCH_3$ (I) to the overall reaction is more important than that of $CF_2HCOOCH_3$ (II). For example, the values of $k_{1T}/k_{overall}$ are 0.61 at 200 K and 0.55 at 250 K, respectively. However, as the temperature increases, $CF_2HCOOCH_3$ (II) prevails over $CF_2HCOOCH_3$ (I) and then becomes the major one, with the ratio of k_{2T}/k_T 0.60 at 1000 K.

The overall rate constants and the rate constants as well as weight factors for each conformer are presented in Table 2, along with the available experimental value [8]. It is seen that the calculated dual-level ICVT/SCT rate constant of $k = 6.06 \times 10^{-14}$ cm^3 $molecule^{-1}$ s^{-1} at 298 K is in reasonable agreement with the experimental value of $k = 1.48 \times 10^{-13}$ cm^3 $molecule^{-1}$ s^{-1}, within a factor of 2.5. In general, the effect of fluorine substitution on the C–H bond strengths is attributed to two counteracting electronic effects, i.e., electron-donating conjugative effect and electron-withdrawing inductive effect of F atom [32–34]. According to the electron-donating conjugative effect, F atom donates electron density to the C central weakening the adjacent C–H bond. Our calculated rate constant of the H-abstraction from the $-CCF_2H$ group of $CF_2HCOOCH_3$ is 1.33×10^{-14} cm^3 $molecule^{-1}$ s^{-1} at 298 K, larger than that of 6.56×10^{-15} cm^3 $molecule^{-1}$ s^{-1} [35] from the $-CCH_3$ group of CH_3COOCH_3, showing that fluorine substitution enhances the H-abstraction of the adjacent H atom. On the other hand, the electron-withdrawing inductive effect of F atom makes the adjacent C positively charged, and the positive charge is relayed through σ-bonds in the chain strengthening the vicinal C–H bond. For the $-OCH_3$ group of $CF_2HCOOCH_3$, the rate constant of the H-abstraction is 3.01×10^{-14} cm^3 $molecule^{-1}$ s^{-1} at 298 K, much smaller than that of 3.25×10^{-13} cm^3 $molecule^{-1}$ s^{-1} from the same group of CH_3COOCH_3, consistent with the above analysis. Since the H-abstraction from the $-OCH_3$ group has main contribution to the overall reaction for both $CF_2HCOOCH_3$ and CH_3COOCH_3, the overall rate constant, 6.06×10^{-14} cm^3 $molecule^{-1}$ s^{-1} at 298 K, for the reaction of $CF_2HCOOCH_3$ + OH is smaller than that of 3.41×10^{-13} cm^3 $molecule^{-1}$ s^{-1} from CH_3COOCH_3 [35], which indicates $CF_2HCOOCH_3$ is less reactive than CH_3COOCH_3 in the H-abstraction by OH radical. The fluorine substitution decreases the molecular reactivity, resulting in lower rate constant of $CF_2HCOOCH_3$ toward OH radicals.

Since there is few data available at other temperatures, for providing theoretical prediction for the title reaction, the three-parameter fits for k_1, k_2, and $k_{overall}$ within 200–1000 K are given as follows (in cm^3 $molecule^{-1}$ s^{-1}).

$$k_1 = 4.58 \times 10^{-25}\ T^{4.01}\ \exp(-720/T)$$

$$k_2 = 7.04 \times 10^{-23}\ T^{3.41}\ \exp(-489/T)$$

$$k_{overall} = 7.31 \times 10^{-24}\ T^{3.68}\ \exp(-551/T)$$

5. Conclusions

In this paper, dual-level direct dynamics method is employed in the study of the hydrogen abstraction reactions of $CF_2HCOOCH_3$ + -OH. The electronic structure calculations are carried out at the M06-2X/aug-cc-pVDZ level and high-level energies of the stationary points and the points selected on the MEP are calculated at the MCG3-MPWB//M06-2X level. The theoretical rate constants are calculated in the temperature range from 200 K to 1000 K by improved canonical variational transition-state theory (ICVT) with the small-curvature tunneling (SCT) correction. The reactant $CF_2HCOOCH_3$ has two stable conformers, $CF_2HCOOCH_3$ (I) with C_s symmetry more stable than $CF_2HCOOCH_3$ (II) with C_1 symmetry by 0.48 kcal mol^{-1}, and as a result, the overall rate constants are considered by the contribution of the two conformers total rate constants. For each conformer, the H-abstraction channels from the $-CH_3$ and $-CF_2H$ groups are identified. For $CF_2HCOOCH_2$ (I), there are two channels from $-CH_3$ group and one from $-CF_2H$ group, and for $CF_2HCOOCH_3$ (II), there are three distinguished H-abstractions channels from $-CH_3$ group and two distinguished H-abstractions channels from $-CF_2H$ group. The present calculations suggest that for $CF_2HCOOCH_2$ (I), the H-abstraction reactions mainly take place at the $-CH_3$ group over the whole temperature range, and for $CF_2HCOOCH_3$ (II), the H-abstractions from the $-CH_3$ group are the major channels at low temperature, while the H-abstractions from the $-CF_2H$ group become more important than those from $-CH_3$ group with the increasing of temperature. Theoretical results show reasonable agreement with the available experimental data. The three parameter expressions for each conformer and the overall reaction within 200–1000 K are $k_1 = 4.58 \times 10^{-25}\ T^{4.01} \exp(-720/T)$, $k_2 = 7.04 \times 10^{-23}\ T^{3.41} \exp(-489/T)$, $k_{overall} = 7.31 \times 10^{-24}\ T^{3.68} \exp(-551/T)$ cm^3 $molecule^{-1}$ s^{-1}, respectively. Furthermore, the enthalpies of formation of $CF_2HCOOCH_3$ (I), $CF_2HCOOCH_3$ (II), $CF_2HCOOCH_2$ (I), $CF_2HCOOCH_2$ (II) and CF_2COOCH_3 are evaluated by using isodesmic reactions at the MCG3-MPWB//M06-2X/aug-cc-pVDZ level.

Acknowledgements

We thank Professor Donald G. Truhlar for providing the POLYRATE 9.7 program. This work is supported by the National Nature Science Foundation of China (20973077, and 21373098) and the Program for New Century Excellent Talents in University (NCET).

Appendix A. Supplementary material

Supplementary data associated with this article can be found, in the online version, at http://dx.doi.org/10.1016/j.comptc.2013.12.019.

References

[1] M.J. Molina, F.S. Rowland, Stratospheric sink for chlorofluoromethanes: chlorine atomic-catalysed destruction of ozone, Nature 249 (1974) 810–812.
[2] R.E. Rebber, P.J. Ausloos, Photodecomposition of $CFCl_3$ and CF_2Cl_2, J. Phtotchem. 4 (1975) 419–434.
[3] J.K. Hammitt, F. Camm, P.S. Connell, W.E. Mooz, K.A. Wolf, D.J. Wuebbles, A. Bamezoi, Future emission scenarios for chemicals that may deplete stratospheric ozone, Nature 330 (1987) 711–716.
[4] R.E. Rebber, P.J. Ausloos, A flash photolytic study of the photo-oxidation of some inorganic anions by the uranyl ion, J. Phtotchem. 6 (1976) 265–275.
[5] M.P. Sulbaek Andersen, O.J. Nielsen, T.J. Wallington, M.D. Hurley, G.W. DeMoore, Atmospheric chemistry of $CF_3OCF_2CF_2H$ and $CF_3OC(CF_3)_2H$: reaction with Cl atoms and OH radicals, degradation mechanism, global warming potentials, and empirical relationship between k(OH) and k(Cl) for organic compounds, J. Phys. Chem. A 109 (2005) 3926–3934.
[6] L. Chen, K. Kutsuna, K. Tokuhashi, A. Sekiya, R. Tamai, Y. Hibino, Kinetics and mechanism of $(CF_3)_2CHOCH_3$ reaction with OH radicals in an environmental reaction chamber, J. Phys. Chem. A 109 (2005) 4766–4771.
[7] L. Chen, K. Kutsuna, K. Tokuhashi, A. Sekiya, Kinetics and mechanisms of $CF_3CHFOCH_3$, $CF_3CHFOC(O)H$, and $FC(O)OCH_3$ reactions with OH radicals, J. Phys. Chem. A 110 (2006) 12845–12851.
[8] M.B. Blanco, M.A. Teruel, Atmospheric degradation of fluoroesters (FESs): gas-phase reactivity study towards OH radicals at 298 K, Atmos. Environ. 41 (2007) 7330–7338.
[9] M.B. Blanco, I. Bejan, I. Barnes, P. Wiesen, M.A. Teruel, Kinetics of the reactions of chlorine atoms with selected fluoroacetates at atmospheric pressure and 298 K, Chem. Phys. Lett. 453 (2008) 18–23.
[10] D.G. Truhlar, in: D. Heidrich (Ed.), The Reaction Path in Chemistry: Current Approaches and Perspectives, Kluwer, Dordrecht, The Netherlands, 1995, p. 229.
[11] W.P. Hu, D.G. Truhlar, Factors affecting competitive ion-molecule reactions: $ClO^- + C_2H_5Cl$ and C_2D_5Cl via E2 and S_N2 channels, J. Am. Chem. Soc. 118 (1996) 860–869.
[12] D.G. Truhlar, B.C. Garrett, S.J. Klippenstein, Current status of transition-state theory, J. Phys. Chem. 100 (1996) 12771–12800.
[13] Y. Zhao, D.G. Truhlar, The M06 suite of density functionals for main group thermochemistry, thermochemical kinetics, noncovalent interactions, excited states, and transition elements: two new functionals and systematic testing of four M06-class functionals and 12 other functionals, Theor. Chem. Acc. 120 (2008) 215–241.
[14] Y. Zhao, D.G. Truhlar, Multicoefficient extrapolated density functional theory studies of $\pi\cdots\pi$ interactions: the benzene dimer, J. Phys. Chem. A 109 (2005) 4209–4212.
[15] D.G. Truhlar, B.C. Garrett, Variational transition-state theory, Acc. Chem. Res. 13 (1980) 440–448.
[16] D.G. Truhlar, B.C. Garrett, Variational transition state theory, Annu. Rev. Phys. Chem. 35 (1984) 159–189.
[17] D.G. Truhlar, A.D. Isaacson, B.C. Garrett, Generalized transition state theory, in: M. Baer (Ed.), The Theory of Chemical Reaction Dynamics, vol. vol 4, CRC Press, Boca Raton, 1985, p. 65.
[18] Y.Y. Chuang, J.C. Corchado, D.G. Truhlar, Mapped interpolation scheme for single-point energy corrections in reaction rate calculations and a critical evaluation of dual-level reaction path dynamics methods, J. Phys. Chem. A 103 (1999) 1140–1149.
[19] M.J. Frisch, et al., GAUSSIAN 09, Rev. A.1, Gaussian Inc., Wallingford, CT, 2009.
[20] J.C. Corchado, Y.Y. Chuang, P.L. Fast, W.P. Hu, Y.P. Liu, G.C. Lynch, K.A. Nguyen, C.F. Jackels, A.F. Ramos, B.A. Ellingson, B.J. Lynch, V.S. Melissas, J. Villa, I. Rossi, E.L. Coitino, J. Pu, T.V. Albu, R. Steckler, B.C. Garrett, A.D. Isaacson, D.G. Truhlar, POLYRATE, Version 9.7., University of Minnesota, Minneapolis, MN, 2007.
[21] B.C. Garrett, D.G. Truhlar, R.S. Grev, A.W. Magnuson, Improved treatment of threshold contributions in variational transition-state theory, J. Phys. Chem. 84 (1980) 1730–1748.
[22] D.H. Lu, T.N. Truong, V.S. Melissas, G.C. Lynch, Y.P. Liu, B.C. Grarrett, R. Steckler, A.D. Issacson, S.N. Rai, G.C. Hancock, J.G. Lauderdale, T. Joseph, D.G. Truhlar, POLYRATE 4: a new version of a computer program for the calculation of chemical reaction rates for polyatomics, Comput. Phys. Commun. 71 (1992) 235–262.
[23] Y.P. Liu, G.C. Lynch, T.N. Truong, D.H. Lu, D.G. Truhlar, B.C. Garrett, Molecular modeling of the kinetic isotope effect for the [1,5] sigmatropic rearrangement of cis-1,3-pentadiene, J. Am. Chem. Soc. 115 (1993) 2408–2415.
[24] M. Taghikhani, G.A. Parsafar, H. Sabzyan, Theoretical investigation of the hydrogen abstraction reaction of the OH radical with CH_3CHF_2 (HFC152-a): a dual level direct density functional theory dynamics study, J. Phys. Chem. A 109 (2005) 8158–8167.
[25] A. Galano, J.R. Alvarez-Idaboy, M.E. Ruiz-Santoyo, A. Vivier-Bunge, Mechanism and kinetics of the reaction of OH radicals with glyoxal and methylglyoxal: a quantum chemistry + CVT/SCT approach, ChemPhysChem 5 (2004) 1379–1388.
[26] Y. Wang, J.Y. Liu, L. Yang, X.L. Zhao, Y.M. Ji, Z.S. Li, Direct dynamics studies on hydrogen abstraction reactions of CH_3CHFCH_3 and $CH_3CH_2CH_2F$ with OH radicals, J. Phys. Chem. A 111 (2007) 7761–7770.
[27] T.Y. Jin, C.G. Ci, Y. Wu, J.Y. Liu, Theoretical studies on mechanism and kinetics of the hydrogen-abstraction reaction of $CF_3CH_2CH_2OH$ with OH radical, Comput. Theor. Chem. 1007 (2013) 63–75.
[28] L.X. Feng, J. Jia, A. Wang, Y.K. Wang, Direct dynamics study on the hydrogen abstraction reaction of fluoromethanes with vinyl radical, Comput. Theor. Chem. 1020 (2013) 143–150.
[29] X.L. Zhao, B. Niu, L. Sheng, Branching ratio of gas-phase reaction of $CH_3C(O)CHCl_2$ + OH: a theoretical dynamic study, Comput. Theor. Chem. 1008 (2013) 61–66.
[30] IUPAC. <http://www.iupac.org/reports/1999/7110minkin/i.html>.
[31] P.J. Linstrom, W.G. Mallard (Eds.), Chemistry Webbook NIST. <http://webbook.Nist.Gov/chemistry>.
[32] Y.G. Lazarou, P. Papagiannakopoulos, Theoretical investigation of the thermochemistry of hydrofluoroethers, Chem. Phys. Lett. 301 (1999) 19–28.
[33] A.K. Chandra, T. Uchimaru, The C–H bond dissociation enthalpies of haloethers and its correlation with the activation energies for hydrogen abstraction by OH radical: a DFT study, Chem. Phys. Lett. 334 (2001) 200–206.
[34] V.C. Papadimitriou, K.G. Kambanis, Y.G. Lazarou, P. Papagiannakopoulos, Kinetic study for the reactions of several hydrofluoroethers with chlorine atoms, J. Phys. Chem. A 108 (2004) 2666–2674.
[35] L. Yang, J.Y. Liu, Z.S. Li, Theoretical studies of the reaction of hydroxyl radical with methyl acetate, J. Phys. Chem. A 112 (2008) 6364–6372.